Monte Carlo Study of the Second Virial Coefficient and Statistical Exponent of Star Polymers with Large Numbers of Branches

Kazuhito Shida,*,† Kaoru Ohno,† Masayuki Kimura,‡ and Yoshiyuki Kawazoe†

Institute for Materials Research, Tohoku University, Sendai 980-8577, Japan; and Japan Advanced Institute of Science and Technology, Asahidai, Tatsunokuchi-machi, Nomi-gun, Ishikawa 901-21, Japan

Received May 12, 1999; Revised Manuscript Received June 26, 2000

ABSTRACT: Computer simulations on the self- and mutual-avoiding effects of two star polymers in a good solvent are reported where the number f of the branches has been extended to the region where no experimental results are yet available. A simple and efficient Monte Carlo (MC) sampling technique was used for the lattice-model simulations. Calculations were performed for 8- to 24-arm star polymers, which complement our previous work and also Rubio et al.'s off-lattice MC simulations. The radius of gyration, the total number of configurations, and its exponent $\gamma(f)$ are evaluated. The values of $\gamma(f)$ obtained are consistent with the large f behavior $\sim f^{3/2}$ predicted by Ohno (*Phys. Rev.* **1989**, *A40*, 1424). The pair-distribution function, the second virial coefficient, and the penetration function are also evaluated. The first order ϵ-expansion, which is a naive approximation of the penetration function, has been known to become increasingly inaccurate for large f. The results of the simulations give further confirmation of the inaccuracy.

I. Introduction

Studying various properties of solution of flexible polymer brings us an important and fundamental understanding in complex polymer systems.[1]

In particular, the star polymers in good solvents show simple but interesting scaling behaviors of several statistical properties. The star polymers are polymers consisting of more than two chains, which are called arms, all starting from a center base. The star polymers are now realized by advancement of polymer synthesis technology with rather precise control of their number of arms and the length of each arm. The star polymers are also related to other subjects such as colloidal particles with many polymer chains adsorbed on their surface[2] and micelles formed by block copolymers.[3]

Assuming the star polymers are at the good-solvent limit, one of the most important physical quantities of such systems is the total number of the configurations, N. Since every configuration has the same internal energy at the good-solvent limit, the number of the configurations has a large effect on the behavior of polymer chains through the entropic effect.

The same entropic effect can be calculated by the classical Flory−Huggins approximation[4−6] in a form of the mixing entropy. However, it does not work well in the dilute regime, because of the existence of strong fluctuations of the polymer concentration, c.

The scaling theory, which has been successful for predicting various physical quantity of polymer systems,[6,7] cannot predict an explicit form of the free energy as a function of c. Therefore, when one wants to investigate the interaction between star polymers, which is synonymous with the dependence of system's free energy on the polymer concentration, analytical approaches such as the renormalization-group method[8−11] or numerical approaches such as Monte Carlo simulations[12−21] should be introduced. In particular, lattice Monte Carlo (LMC) simulations, using self-avoiding walks (SAWs) as a model of polymers with the excluded volume effect (EVE), is a powerful tool to study the dilute regime, because it can estimate N directly, as well as various basic parameters of the polymers as follows.

For an isolated star with f arms each of which have l segments, N is characterized by the effective coordination number μ and an f-dependent critical exponent $\gamma^{\mathrm{eff}}(f)$ as

$$N \sim l^{\gamma^{\mathrm{eff}}(f)-1}\,\mu^{fl} \tag{1.1}$$

Deciding the f dependence of $\gamma^{\mathrm{eff}}(f)$ is an interesting problem of statistical physics in its relationship with spin systems.[22] Of course, N and the free energy of an isolated star are useful for calculating those of the entire solution.

Also conformational properties[4,5,23−25] such as the gyration radius or the virial coefficients are of interest and importance, which deviate systematically from those of linear polymer as functions of f.

The mean square radius of gyration, $\langle r^2\rangle_{\mathrm{g}}$, is a measure of the intra-star EVE, which behaves as[10,11,26]

$$\langle r^2\rangle_{\mathrm{g}} = \frac{1}{2(N+1)^2}\sum_{i=0}^{N}\sum_{j=0}^{N}\langle(\mathbf{r}_i-\mathbf{r}_j)^2\rangle \simeq c(f)l^{2\nu},$$
$$c(f)\sim f^{1-\nu},\quad f\to\infty \tag{1.2}$$

where ν is the correlation-length exponent, which is the same as the corresponding value for a linear chain;[7] for $d = 3$, $\nu = 0.59$.

On the other hand, the second virial coefficient A_2 serves as a measure of the inter-star EVE in the dilute regime of polymer solutions. Basically, the second virial coefficient A_2 is related to the osmotic pressure Π of a dilute solution of monodisperse star polymers. In the dilute limit, Π is expressed by a power series of the concentration c as

† Tohoku University.
‡ Japan Advanced Institute of Science and Technology

10.1021/ma990746l CCC: $19.00
Published on Web 09/08/2000

$$\frac{\Pi}{N_A k_B T} = \frac{c}{M} + A_2 c^2 + A_3 c^3 + \ldots \qquad (1.3)$$

where N_A is Avogadro's number, and M the molecular weight of a polymer. This series is a virial expansion, and A_i ($i = 2, 3, \ldots$) is the ith virial coefficient of the solution. Available experimental information about the virial coefficients is mostly limited to A_2, because of the difficulty of the estimation of A_3 and the higher virial coefficients.[27,28] Since the osmotic pressure can be obtained by differentiation of the free energy with respect to the volume of the solution, the virial coefficients are also related to the free energy.

Let us consider polymers in a dilute solution, assuming only two star polymers at a time, and introduce an expression for the A_2 by means of the positions of segments. Let $\mathbf{r}_i$ (or $\mathbf{s}_i$) denote the end point of the ith segment of the first (or second) star polymer, and $\mathbf{r}_0$ (or $\mathbf{s}_0$) denote the position of the center of the first (second) star polymer. By means of the two-body interaction $u(\mathbf{r}_i - \mathbf{s}_j)$ between two segments i and j of the first and second star polymers, one can express the second virial coefficient A_2 as

$$A_2 = -\frac{N_A}{2V M^2}\int\int P(\{\mathbf{r}\})P(\{\mathbf{s}\})\{\exp[-\beta\sum_{i=0}^{N}\sum_{j=0}^{N}u(\mathbf{r}_i - \mathbf{s}_j)] - 1\}\prod_{k=0}^{N} d\mathbf{r}_k\, d\mathbf{s}_k \qquad (1.4)$$

where V is the volume of the solution, $\beta = 1/k_B T$, and $P(\{\mathbf{r}\})$ is the one-body distribution function of a star polymer normalized as

$$\int P(\{\mathbf{r}\})\prod_{k=1}^{N} d\mathbf{r}_k = 1 \qquad (1.5)$$

The penetration function Ψ

$$\Psi = \frac{A_2 M^2}{4\pi^{3/2} N_A \langle r^2\rangle_g^{3/2}} \qquad (1.6)$$

which is a function of the second virial coefficient and the mean-square radius of gyration, is known to be a universal quantity in the long-chain limit. The penetration function can be used in both theoretical studies and experimental analyses, which is very useful for making comparison between them.

In the present paper, we will extend our previously reported LMC simulations of star polymers[20] toward the limit of large f. For the case of $8 \le f \le 12$, this is carried out just by increasing the number of the arms in the same framework of simulation we used before. The effect of asymmetry incorporated by increasing the number of arms is minimized by increasing the maximum contour length of each arm accordingly to $l = 160$. The methods have, however, a problem of degrading efficiency of sample generation when the number of the arms are large. A new way of calculation is devised to avoid this problem by using another approximation which simulates the two-bodies interaction indirectly. The new calculation technique is employed for the simulation runs for $12 < f \le 24$. In this case too, the maximum length of each arm is set to 160.

In summary, we calculate (1) the radius of gyration of an isolated star polymer, (2) assuming the dilute solution limit, the total number of configurations of two star polymers as a function of f, l, and the distance between the stars D, (3) the pair-distribution function $g(l,D)$ of star polymers in the dilute solution limit, which is related to the inter-star potential, and (4) the second virial coefficient and the penetration function obtained from $g(l,D)$.

The paper is organized as follows: In section 2, we review the algorithm used for $f < 12$. In section 3, the modification on the algorithm for star polymers with large numbers of arms is described. Numerical results are presented in section 4, and section 5 contains our conclusions and discussions.

II. Algorithm

Using an enrichment algorithm[12−15] on the basis of a simple Monte Carlo sampling technique, we generate a large number of samples of two f-arm star polymers with their center bases D apart. Each sample has a total of $2f$ arms.

In the enrichment algorithm, we generate $2f$ arms each having the same length l (the "lth generation") from a preexisting sample having $2f$ arms but with the length $l - 1$ (the "$(l - 1)$th generation"). The number of arms, $2f$, is fixed throughout a simulation run. In the present study, the first-generation corresponding to $l = 1$ is obtained by assuming the fixed directions of all the $2f$ segments. On a simple cubic lattice, discarding the sixth direction in which the arm would fold backward on itself, we have five ways of elongating one end of each arm by one segment. At each step of creating the next generation, the self-avoidance condition is tested; unless this condition is fulfilled, the newly generated configuration is discarded. Thus, if we want to obtain all possible realizations of the lth generation samples from the M_{l-1} distinct realizations at the $(l - 1)$th generation, we have to make $5^{2f} M_{l-1}$ trials (5^{2f} trials for each realization of the $(l - 1)$th generation) and discard the nonphysical realizations which violate the self-avoidance condition. The expected number M_l' of accepted configurations out of the full number of trial configurations $5^{2f} M_{l-1}$ is given by

$$\frac{M_l'}{M_{l-1}} = \frac{N(l,D)}{N(l-1,D)} = \mu^{2f} \qquad (2.1)$$

where $\mu = 4.6838$ is the effective coordination number for self-avoiding walks on the simple cubic lattice.[29] The full $5^{2f} M_{l-1}$ trials are not necessary. To maintain a sufficient number of samples $M_{l-1} \approx M_l \approx M_{l+1} \approx \ldots$ for acceptably small statistical error up to some given maximum of l, much less, say $m M_{l-1}$($m \ll 5^{2f}$), Monte Carlo trials are enough. The condition $M_l/M_{l-1} \ge 1$ is satisfied when we choose $m \ge (5/\mu)^{2f} = (1.0675)^{2f}$. For f as large as $f = 6$, a very small value of m ($\approx$2.2) results. In practice, it is better to work with somewhat larger values of m for small l. The value of m may be controlled automatically so that the number of samples will gradually increases as the arm length l increases. Such increasing of the sample size is necessary for avoiding an nonphysical "bias" caused by the iteration. Regardless of the value of m, this enrichment algorithm for star polymers significantly reduces the computational time.

Since the actual number of trial configurations made is mM_{l-1} instead of $5^{2f} M_{l-1}$, we have

$$\frac{M_l}{M_{l-1}} = \frac{M_l' \; m}{M_{l-1}5^{2f}} = m\left(\frac{\mu}{5}\right)^{2f} \tag{2.2}$$

Combining eqs 2.1 and 2.2, we see that the particular value of the ratio M_l/M_{l-1} yields the desired information on the ratio of the subsequent total numbers of configurations:

$$\frac{N(l,D)}{N(l-1,D)} = \frac{5^{2f} M_l}{mM_{l-1}} \tag{2.3}$$

The subsequent total-number ratio can be evaluated straightforwardly from eq 2.3. The total-number ratio in eq 2.3 is related to the effective value for the configuration-number exponent $\gamma^{\text{eff}}(f)$. The total number of configurations for large l has an asymptotic behavior

$$N(l,D) \sim \begin{cases} l^{2\gamma^{\text{eff}}(f)-2}\mu^{2fl}, & \text{for } D \to \infty, \\ l^{\gamma^{\text{eff}}(2f)-1}\mu^{2fl}, & \text{for } D \to 0. \end{cases} \tag{2.4}$$

Thus, we have

$$\frac{N(l,\mathrm{D})}{N(l-1,\mathrm{D})} = \begin{cases} \mu^{2f}\left[1 + \dfrac{2\gamma^{\text{eff}}(f)-2}{l} + O\left(\dfrac{1}{l^2}\right)\right], & \text{for } D \to \infty \\ \mu^{2f}\left[1 + \dfrac{\gamma^{\text{eff}}(2f)-1}{l} + O\left(\dfrac{1}{l^2}\right)\right], & \text{for } D \to 0 \end{cases} \tag{2.5}$$

or, by taking its ($^1/_2f$)th power

$$\left[\frac{N(l,D)}{N(l-1,D)}\right]^{1/2f} = \begin{cases} \mu\left[1 + \dfrac{\gamma^{\text{eff}}(f)-1}{fl} + \mathrm{O}\left(\dfrac{1}{l^2}\right)\right], & \text{for } D \to \infty \\ \mu\left[1 + \dfrac{\gamma^{\text{eff}}(2f)-1}{2fl} + O\left(\dfrac{1}{l^2}\right)\right], & \text{for } D \to 0 \end{cases} \tag{2.6}$$

Consequently, the configuration-number exponent $\gamma^{\text{eff}}(f)$ is determined by plotting $[N(l,D)/N(l-1,D)]^{1/2f}$ vs $1/fl$ for large l. Of course, a similar procedure can be used for estimating $\gamma^{\text{eff}}(f)$ from N of an isolated star.

In a Monte Carlo simulation based on the enrichment algorithm, one can evaluate directly the successive ratios $\{N(l,D)/N(l-1,D)\}$. If we multiply these successive ratios from $\{N(10,D)/N(9,D)\}$ to $\{N(l,D)/N(l-1,D)\}$ (where $l \gg 10$), for example, we have

$$\frac{N(l,D)}{N(9,D)} = \frac{N(l,D)}{N(l-1,D)}\frac{N(l-1,D)}{N(l-2,D)}\cdots\frac{N(11,D)}{N(10,D)}\frac{N(10,D)}{N(9,D)} \tag{2.7}$$

Then, dividing this function by the same function, but with $D = \infty$, we obtain the pair-distribution function in the dilute limit:

$$g(l,D) = \frac{N(l,D)}{N(l,\infty)} = \frac{N(l,D)}{N(9,D)}\frac{N(9,\infty)}{N(l,\infty)} = \frac{\dfrac{N(l,D)}{N(l-1,D)}\cdots\dfrac{N(10,D)}{N(9,D)}}{\dfrac{N(l,\infty)}{N(l-1,\infty)}\cdots\dfrac{N(10,\infty)}{N(9,\infty)}} \tag{2.8}$$

In deriving the second equality, we used $N(9,D) = N(9,\infty) = N^2(9)$ for sufficiently large D (in fact this relation holds for all D satisfying $D > 18$).

In the expression of the second virial coefficient A_2 of eq 1.4, usually the two body interaction $u(\mathbf{r}_i - \mathbf{s}_j)$ is approximated by $(\alpha/\beta)\delta(\mathbf{r}_i - \mathbf{s}_j)$ with an EVE parameter α. Furthermore, in a lattice model, all the spatial integrals are replaced by summations over all lattice points, and the exponential is replaced by

$$\exp[-\alpha\sum_{i=0}^{N}\sum_{j=0}^{N}\delta(\mathbf{r}_i - \mathbf{s}_j)] \to \prod_{i=0}^{N}\prod_{j=0}^{N}(1 - \delta_{\mathbf{r}_i,\mathbf{s}_j}) \tag{2.9}$$

We notice that the total number of configurations $N(l,D)$ of two star polymers separated by a distance $\mathbf{D} = \mathbf{r}_0 - \mathbf{s}_0$ is expressed as

$$N(l,D) = N(l)^2\sum_{\{\mathbf{r}\}}\sum_{\{\mathbf{s}\}}P(\{\mathbf{r}\})\mathrm{P}(\{\mathbf{s}\})\delta_{\mathbf{r}_0,\mathbf{s}_0+\mathbf{D}}\prod_{i=0}^{N}\prod_{j=0}^{N}[1 - \delta_{\mathbf{r}_i,\mathbf{s}_j}] \tag{2.10}$$

where $N(l)$ denotes the total number of configurations of an isolated star polymer. Substituting eq 2.10 in eq 1.4, we find the relation between the second virial coefficient and the pair-distribution function in the dilute limit

$$\frac{A_2M^2}{N_{\mathrm{A}}} = -\frac{1}{2}\int\{g(l,D) - 1\}\,\mathrm{d}\mathbf{D} \tag{2.11}$$

Here we used a relation indicating an absence of the interference at $D = \infty$, i.e., $N(l)^2 = N(l,\infty)$. The function approaches zero for small D and goes to unity for large D.

Finally, by substituting eq 2.8 in eq 2.11, we can evaluate the second virial coefficient from the subsequent ratios of the total number of configurations. This is an outline of the method used in our previous work.[20] In this paper, we refer to this as "method A". By method A, 8- to 12-arm star polymers are simulated. The $g(l,D)$ and the A_2 are calculated for 8- and 12- arm star polymers.

III. Enrichment Algorithm for a Larger Number of Arms

The enrichment algorithm needs mM_{l-1} Monte Carlo trials for each elongation step. When two-body interaction of stars is the subject, the condition $m \geq (5/\mu)^{2f} = (1.0675)^{2f}$ should be satisfied. This means that although m is a sufficiently small value for small f, it is a fast increasing function of f and soon the computational load will be intractably large.

An improvement of the enrichment algorithm is introduced for such a case: the ensemble is generated for single star polymer when large f is required. Then pairs of the stars are created by selecting two stars randomly from the ensemble and combining them so

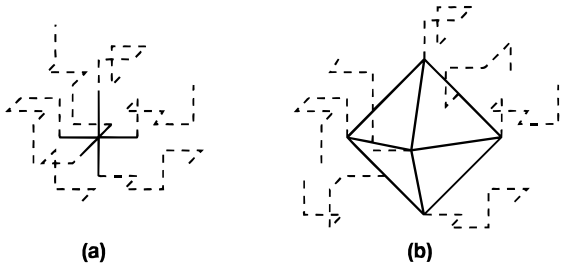

Figure 1. Since a simple cubic lattice is employed, (a) a lattice site was used for the center base for the case of $f \leq 6$, and (b) a polyhedron with finite size and internal space is necessary for the case of $f > 6$.

that their center bases are D apart. the two-body interactions are calculated for each of the pairs, eliminating pair configurations with colliding segments. The effect of inter-star EVE is taken into account by checking of colliding segments between different stars by means of a simple hash-table searching algorithm. By counting the star pairs without such collision, the total configuration number N of star pairs with a given D is estimated.

Such a simplification is equivalent to an approximation that internal configuration of a star is independent of the other star's internal configuration even if their regions are penetrating each other. This is a fairly natural assumption.

As well as the case of small f, $g(l,D)$ can be calculated from N as a function of D between the elongation steps. In this paper, we refer to this as "method B". By method B, up to 24-arm star polymers are simulated. The $g(l,D)$ and the A_2 are calculated for 18- and 24- arm star polymers.

The only remaining issue on the algorithm is how to prepare the center base. For the case of $f \leq 6$, the center base was just a lattice site as shown in part a of Figure 1. Once f is larger than 6, a polyhedron must be used as the center base. The polyhedral center bases, as shown in part b of Figure 1, have three problems. First, the vacant sites on the surface of center bases give rise to an asymmetry. Second, its finite size can effect on conformational properties of the stars. Third, we need another treatment for the inside of the center bases. For example, we must decide whether the inside is filled with segments or is left hollow. These issues will be discussed in the following section.

IV. Results

We performed simulations by method A first. For each case of f, we evaluated the subsequent ratio $N(l,D)/N(l-1,D)$ of the total number of configurations for $l = 1-160$. For the value of D, multiples of 10 are sampled. The minimum value of D must be a distance at which two stars have always overlapping. That is, all generated sample configuration has overlapping segments at the minimum distance. The selected minimum value is $D = 10$. The maximum value of D must be a distance at which two stars have no interactions. This is decided according to the data of $\langle r^2 \rangle_g$. The maximum D sampled is $D = 100$. Later, the legitimacy of these selection of D will be checked by obtained $g(l,D)$. The number of the star samples is roughly 100 000 in each case of method A.

When method B was used, the condition about l was not changed from the case of method A. However, we had to reduce the number of the star samples to about one-tenth of that in the case of method A. Since 6 (for the case of $f = 24$) to 10 "opponent" stars are chosen from the same ensemble, this condition corresponds to an ensemble of about 60 000 to 100 000 star pairs. For selecting D, we select 17 different D values (5, 6, 7, 8, 9, 10, 12, 14, 16, 18, 20, 25, 30, 35, 40, 45, 50) in the simulation and assume that $g(l,0) = 0.0$, $g(l,100) = 1.0$. The basic policy, being the same as the case of method A, is satisfied by this selection while the statistics of values of $g(l,D)$ is improved. In addition, several simulation runs for isolated single star in the cases of $f = 8$, 12, 14, 16, 18, 20, and 24 are performed to obtain $\langle r^2 \rangle_g$ and γ^{eff}.

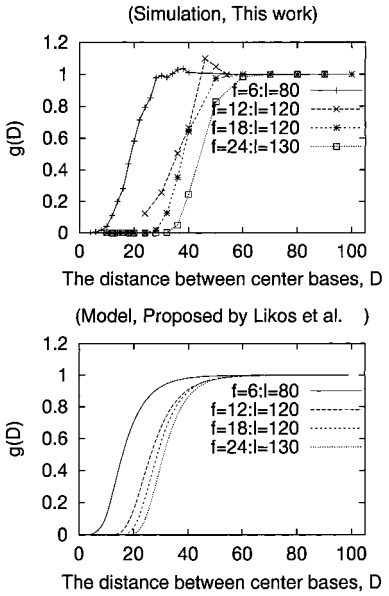

Figure 2. Plot of the pair-distribution function $g(l,D)$ vs D for various l and f values in the dilute limit. Up to the case of $f = 12$, method A was used. The large fluctuation of $g(l,D)$ obtained by method A was canceled by using a smoothing formula, eq 4.2. Also, in the lower half, the result of the model calculation of $g(l,D)$ based on Likos et al.[2] is presented.

First, it should be checked that assumptions and approximations used for improving efficiency of the simulation do not cause any harmful statistical artifact in the simulation. In Figure 2, we show the pair-distribution functions for several f settings. The selection of sample number and the region of D seems to be correct according to these smooth profile and nice convergence to both ends of the abscissa.

Likos et al.[2] have proposed a model on the pair potential based on neutron-scattering experiments on star polymers with large f. The lower half of Figure 2 shows the pair-distribution function calculated by the model. The model gives the $g(D)$ for given overlapping radius, which is assumed to be equivalent to $\langle r^2 \rangle_g^{1/2}$ in the plot. It seems these two plots match very well.

Also, in Figure 3, the pair-distribution functions obtained by methods A and B are compared for a case of the same small number of f (=6). There are only small differences between them. For example, when measured by A_2, the result of method B for $f = 6$, $l = 60$ is 7.2% larger than that of method A. The result of method B for $f = 6$, $l = 80$ is only 1.5% larger than that of method A. However, it is also clear that the result of method A

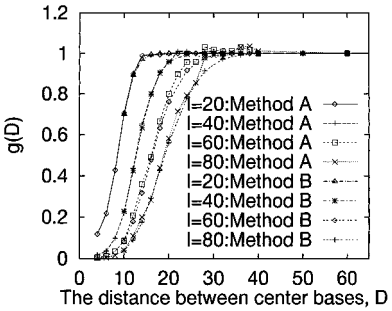

Figure 3. Plot of the pair-distribution function of the 6-arm stars for $l = 20$, 40, 60, and 80 obtained by both of method A and method B of Monte Carlo simulation.

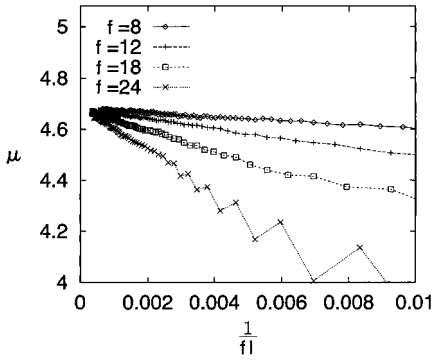

Figure 4. Plot of $[N(l,D)/N(l-1,D)]^{1/f}$ vs $1/f$ for isolated 8-, 12-, 18-, and 24-arm stars. All data approach $\mu = 4.6838$ in the limit $1/fl \rightarrow 0$. The slope of the data is related to the effective configuration-number exponent γ^{eff}.

Table 1. Effective Coordination Number Exponents $\gamma^{\text{eff}}(f)$ Obtained from the Slopes of Data in Figure 4

no. of arms per star	γ
$f = 3$	1.02[a]
$f = 6$	0.07[a]
$f = 8$	−1.00
$f = 12$	−3.35
$f = 14$	−4.94
$f = 16$	−5.90
$f = 18$	−8.12
$f = 20$	−11.33
$f = 24$	−18.13

[a] Values from a previous work.

shows larger fluctuation and even overshooting into the region of $g > 1.0$. Such a overshooting is nonphysical but possible in the formulation of method A as a result of estimation error involved in N. The main deviation between these results can be regarded as a result of this overshooting. Taking this observation into account, we can conclude that method B is an acceptably nice approximation. Also, it should not be forgotten that, for large f, only method B is realizable with a reasonable computational effort.

The effect of a large center base can be checked by the values of exponent μ and γ^{eff} obtained for isolated stars with f arms. The effective coordination number is plotted vs $1/fl$ in Figure 4 to obtain μ and $\gamma^{\text{eff}}(f)$ as its limiting value at $1/fl = 0$ and its slope, respectively. The effective coordination number μ is, as expected, linearly converging to the limiting value 4.6838 and shows that the effect of finite size of core is negligible in this region of l (roughly corresponding to $l > 10$). The estimated $\gamma^{\text{eff}}(f)$ is tabulated in Table 1. To the best of our knowledge, the value of $\gamma^{\text{eff}}(f)$ has not been calculated

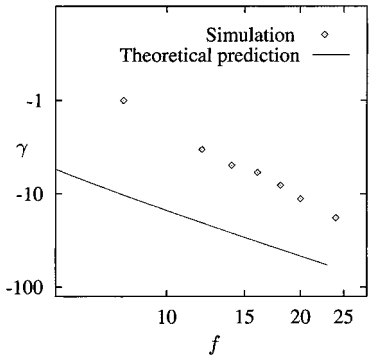

Figure 5. Value of effective configuration-number exponent $\gamma^{\text{eff}}(f)$ obtained by our simulation and the theoretical prediction given by Ohno.[30] To compare their absolute value and power behavior at the same time, the ordinate of the graph is showing $-\log(-\gamma^{\text{eff}})$ while the abscissa is plotted in the usual log manner.

for large f such as $f = 24$ in such a scale of the system. The only exception is ref 14, which treats the case of $f = 32$ using a model similar to ours, but l is limited only up to 50.

We compare our result with a theoretical formula

$$\gamma^{\text{eff}}(f) = 1 + \frac{f}{4} - \frac{3\pi}{16} f^{3/2} \qquad (4.1)$$

predicted by Ohno,[30] by plotting Figure 5. The ordinate of the graph shows $-\log(-\gamma^{\text{eff}})$ while the abscissa is plotted in the usual log manner. The $\gamma^{\text{eff}}(f)$ given by our simulation and the formula are showing large deviation in their absolute values. Since eq 4.1 is given as an asymptotic form at $f \rightarrow \infty$ limit, they would match when f is largely increased. Indeed, it should be noted that the slope of simulation values in Figure 5 is roughly consistent with that of the theory.

Now we turn our attention to the gyration radii of the stars. The gyration radii are calculated for single and isolated stars. Here, we note that there is a hollow region in the center base when $f > 6$. If inside the center base should be filled with the same kind of segments of which the arms are constituted, the gyration radii might be overestimated because the center base must be close to the mass center of the entire star. We have checked this effect by calculating gyration radii of center-filled and center-hollowed stars and found that the difference of gyration-radii caused by above-mentioned effect is at most 1% when $l > 100$. Therefore, we simply assume that there are no segments inside the center base. Obviously, this assumption on the center base has no effect on the pair-distribution function and any other properties related to the interaction between star polymers because entrance of segments into the center base is always prohibited. The amplitude $c(f)$ in eq 1.2 for the radius of gyration is plotted as a function of f on a double logarithmic scales in Figure 6 in the case of $l = 80$ and $l = 100$. This behavior should be compared with the second relation of eq 1.2, which was first derived by Daoud and Cotton,[26] indicated by the straight line in the figure. The agreement between the simulation and the theory are good until $f = 18$. A small deviation which appears in the case of $f = 24$ may be understood as a consequence of the degradation of the number of samples.

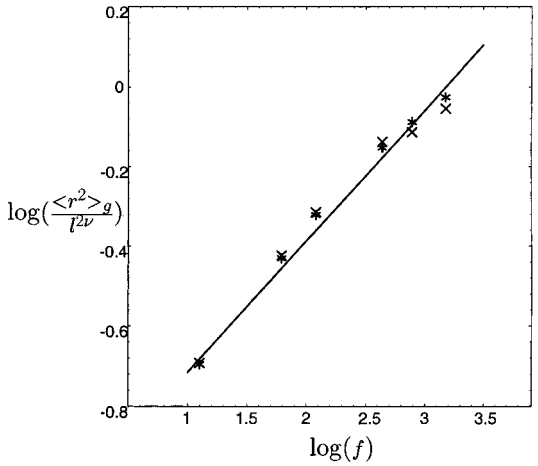

Figure 6. A log−log plot of $\langle r^2\rangle_g/l^{2\nu}$ as a function of f for l = 80 (marked by an asterisk) and l = 130 (marked by ×). The straight line indicates the Daoud and Cotton prediction, eq 1.2: $\langle r^2\rangle_g/l^{2\nu} \sim f^{(1-\nu)}$.[26]

Table 2. Second Virial Coefficient A_2 and the Penetration Function Ψ, for l up to 160 and f = 8−24

no. of segments per arm, l	$\langle r^2\rangle_g$	A_2M^2/N_A	Ψ
	f = 8		
100	163.8	33619	0.72
120	207.3	52518	0.79
140	246.4	68057	0.79
160	282.2	83416	0.79
	f = 12		
100	184.9	78400	1.40
120	231.0	107133	1.37
140	275.5	131388	1.29
160	324.0	161073	1.24
	f = 18		
100	207.3	93070	1.40
120	252.8	124441	1.39
140	299.2	164840	1.43
160	349.6	215478	1.48
	f = 24		
100	219.0	120550	1.67
130	289.0	196971	1.80
160	372.4	284918	1.78

The pair-distribution function can be fitted to the following expression

$$1 - \exp[-(a_1 D)^{a_2}] \tag{4.2}$$

which is suitable for an analytical integration of eq 2.11; it gives the second virial coefficient as

$$\frac{A_2M^2}{N_A} = 2\pi\Gamma\left(1+\frac{3}{a_2}\right)\frac{1}{3{a_1}^3} \tag{4.3}$$

This procedure is also a nice method for interpolating the distribution function by method A with large fluctuation. For method B, a numerical integration is employed. The calculated values of the second virial coefficient are tabulated in Table 2, together with the values of the radius of gyration of isolated star polymer defined by eq 1.2 and the penetration function defined by eq 1.6.

In our previous paper,[20] the second virial coefficient and the penetration function was obtained only for the cases of f = 3−6 stars. The results were compared with those from experimental and theoretical works. The agreement with experiments at f = 4[31,32] was good while a large difference was found for a theoretical prediction based on the renormalization-group calculation.[9]

Values of the penetration function obtained by experiments are known up to f = 18. These results should be compared with our simulation results. The experimental value for f = 12 is 1.10[33] while our result is 1.24−1.40 for the same number of arms. The value at l = 160, 1.24, may be understood as consistent with the experiment within the extent of the estimation error. However, it should also be considered that f = 12 is the case with the largest f calculated by method A. A large fluctuation and an overshooting are observed in the $g(l,D)$ profile, and this may be affecting our result.

The experimental value for f = 18 is 1.10−1.35,[33−35] while our result is observed to be ranging between 1.4 and 1.48 where l is between 100 and 160. This result is roughly consistent with (but slightly different from) experimental data.

Our simulation results should be compared with other computer simulations. Rubio and Freire[21] have performed simulations based on an off-lattice MC sample generation. Although their values (0.995−1.014 for f = 12 and 1.17−1.25 for f = 18) are closer to the experimental values, one should note that the number of the segments l in each arm is also an important factor. The longer the simulated arms are, the more the data are close to the scaling limit ($l \to \infty$). There is no convincing way to convert the l of an off-lattice model into that of a lattice model without any assumption. However, considering that only four lattice segments are required to form a loop in a polymer chain on the lattice, the length of each arm in our work (up to 160 in number of lattice segments) is far closer to the scaling limit than that in Rubio and Freire's work (up to 16 in the number of off-lattice segments). It is also undeniable that experiments using real polymers may have similar problems concerning the polymer arm length.

Another possibility is that our data are overestimated because of the finite size of the center base. This seems plausible especially for f = 12. In this case, the value of the penetration function is decreasing as l increases, and the asymptote seems to be very close to the value for f = 12 reported by Rubio and Freire.

For f = 24, our value is 1.67−1.80. As far as we know, no experimental data have been published for this case.

Next, we compare our result with the theoretical predictions on the penetration function. To obtain reasonable estimates from the renormalization-group analysis, a resummation procedure[11] is required, otherwise the prediction based on the renormalization-group[9] diverges as shown in Figure 7.

An alternative approach is the so-called cone approximation,[11] which is equivalent to Daoud−Cotton's blob picture.[26,36]

In the cone picture, the mutual penetration of two stars is prohibited, because each arm is strongly confined to its own conical zone. We have introduced[20] an approximated upper limit of 2.13 for the penetration function, which may be readily obtained by this condition on mutual penetration. Another possibility is to compare the penetration function with the value 1.6, which is the value of the penetration function known for a rigid sphere with uniform density. These values are related to a speculation that, in the limit $f \to \infty$, a single star polymer behaves as a rigid sphere of closely packed segments,[37,38] and the penetration function becomes a constant of order unity.

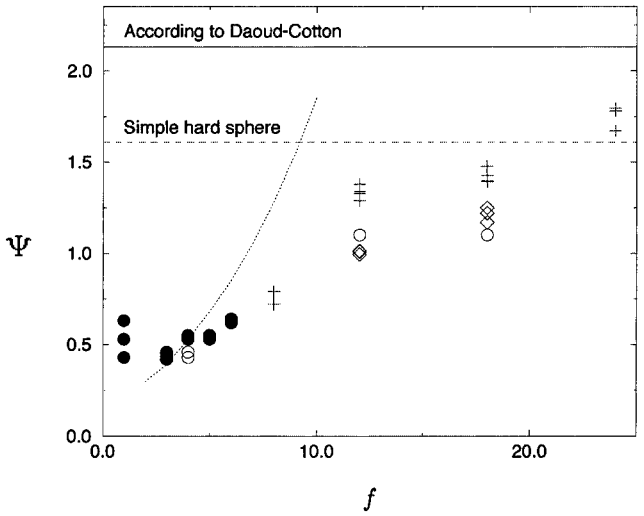

Figure 7. All values of the penetration function so far obtained by computational experiment with several other data for comparison: (+) this work; (◇) Rubio and Freire;[21] (●) our previous work[20] and our result to be published;[39] (○) experiments for $f = 4$,[31,32] $f = 12$,[33] and $f = 18$.[33−35] Curve: renormalization prediction.[9]

All values of the penetration function we have obtained by lattice simulations are shown in Figure 7. The value for linear polymer ($f = 1$),[39] results of other simulation works, and results of experiments are also shown in this figure. It is clear from this figure that the values of our present work are consistent with those of other works. All of them seem to be converging to the value of the Daoud−Cotton-like rigid sphere although their l dependence should be considered too.

Before closing this paper, we want to discuss the possibility of a function which can describe the behavior of the penetration function on wide range of f and l. which can describe the configurational behavior of star polymers on wide range of f and l. Further sophistication of the renormalization-group calculation would be difficult due to higher power terms of f to be incorporated. Because the expected picture for high-f regime is rather simple one like the cone-picture, what is desirable is a handy model which describes a smooth crossover from the star into the cone picture.

Taking this into account, we would like to concentrate on the profile of g and propose a semiempirical model for it. Observing the profile of the pair-distribution function g in Figure 2, one can define the core and the halo regimes of these star polymers in terms of their mutual penetration. At the core regime, the value of g is almost 0, which means mutual penetration of the stars are prohibited at such distance. This regime corresponds to the core regime in Daoud and Cotton's picture,[26] at which the segment density is almost unity. The halo regime is the rest of the star surrounding the core. In this regime, the probability of the mutual penetration is seen to be smoothly decreasing as the distance between stars decreases. Assuming the border between the core and the halo is at $g = 0.03$, we determined the diameter of the core r and plotted it in Figure 8 in double-log manner. Similarly, we determined the halo thickness h, assuming the outside border of the halo is at $g = 0.97$, and plotted it in Figure 9 in double−log manner. Here, the data for $f = 6$ are taken from our previous work[20] representing the behavior of g for smaller f.

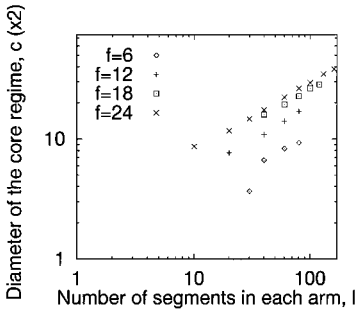

Figure 8. Estimated diameter of the "core" region of the pair-distribution function for $f = 6$, 12, 18, and 24 in a double−log manner suggesting the existence of interesting power-law behavior and an asymptote for larger l. The data for $f = 6$ are from our previous work.[20]

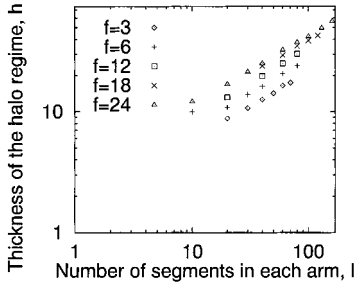

Figure 9. Estimated thickness of the "halo" region of the pair-distribution function for $f = 6$, 12, 18, and 24 in a double−log manner strongly suggesting a power-law behavior. The data for $f = 6$ are from our previous work.

Although these plots are based on arbitrary selected threshold of g, it is rather obvious that there are simple relations in these plots. For the halo regime, a power-law behavior like

$$h = p(f)l^a \tag{4.4}$$

is observed rather clearly. And $p(f)$ is an increasing function of f. It should be noted that the value of a is close to 0.59, that is the exponent characterizing the size of a SAW in three-dimensional lattice. In a sense, this halo regime is behaving like a layer of SAW with one of their ends at the surface of the core region. The form of $p(f)$ is not clear, but in Figure 9, $p(f)$ seems to be close to some asymptotic value already at $f = 24$.

For the core regime, the center base causes a problem. That is, the size of the polyhedral center base in a lattice model shows a steplike increase as the number of the arms increases. Although such an artifact is included in r, it is clear that r behaves largely different from the "core" regime in Daoud and Cotton's theory

$$r = qf^{1/2}l \tag{4.5}$$

It is rather close to

$$r = q(f)l^{0.59} \tag{4.6}$$

and the general tendency is not changed by selecting a different threshold of g. Another point to be noted is that, in Figure 8, $q(f)$ seems to be converging to some asymptote which is larger than that of $p(f)$. This is interesting because when both p and q have reached their asymptote, the core radius and the halo thickness

will be independent of f, and both will scale like $l^{0.59}$. This situation is close to a picture of the arms confined to their own narrow pillarlike region, which extends from a surface outward and is scaled only by length of the arms. This is verily an extreme case of the Daoud−Cotton picture. To confirm this statement, the behavior of p and q must be closely investigated, and it would require a further computational effort. Since $p(f)$ and $q(f)$ give an approximated form of the pair-distribution function g of the stars via eqs 4.4 and 4.6, it is possible to formulate an abstract description of two-body interaction between the stars using $p(f)$ and $q(f)$. However, it is difficult to show that the $p(f)$ and $q(f)$ obtained by present work are free from artifacts like the finite-size effects and the f-dependent size of the center base. Probably, such a formulation requires clearer definition of the core−halo boundary and a better treatment of the center base. Probably, a large scale off-lattice simulation is necessary.

V. Concluding Remarks

In this paper, lattice Monte Carlo simulation is performed and the total number of configurations N, the pair-distribution function in the dilute limit $g(l,D)$, and the second virial coefficient A_2 are obtained. We also estimated the radius of gyration and the configuration number exponent $\gamma^{\text{eff}}(f)$ of isolated stars with various f. Then another approximation is introduced to extend the simulation toward the large f region. The penetration function, as a universal measure of the inter-star repulsion, is estimated for f as large as 24, which has never obtained before. The present result for the penetration function was compared with previous experiments, the cone picture, and the renormalization-group ϵ-expansion studies. Our result significantly deviates from the naive ϵ expansion result, which indicates the necessity of a resummation procedure. A simple model is proposed for the pair-distribution function. Our current results suggests some interesting law between factors in the model.

Acknowledgment. We are grateful to the Information Science Center at JAIST and the Computer Science Group at IMR for their support of computer facilities.

References and Notes

(1) Freire, J. J. *Adv. Polym. Sci.* **1999**, *143*, 35.
(2) Likos, C. N.; Löwen, H.; Watzlawek, M.; Abbas, B.; Jucknischke, O.; Allgaier, J.; Richter, D. *Phys. Rev. Lett.* **1998**, *80*, 4450.
(3) Shida, K.; Ohno, K.; Kawazoe, Y. Abstract of OUMS′ 98 (Osaka University International Exchange Program in Macromolecular Science), 1998, p 29.
(4) de Gennes, P. G. In *Solid State Physics*; Liebert, L., Ed.; Academic Press: New York, 1978; Suppl. 14.
(5) Leibler, L.; Orland, H.; Wheeler, J. C. *J. Chem. Phys.* **1983**, *79*, 3550.
(6) des Cloiseaux, J. *J. Phys.* **1975**, *36*, 281.
(7) de Gennes, P. G. *Scaling Concepts in Polymer Physics*; Cornell University Press: Ithaca, NY, 1979.
(8) Miyake, A.; Freed, K. F. *Macromolecules* **1983**, *16*, 1228; **1984**, *17*, 678.
(9) Douglas, J. F.; Freed, K. F. *Macromolecules* **1984**, *17*, 1854.
(10) Ohno, K.; Binder, K. *J. Phys.* **1988**, *49*, 1329.
(11) Ohno, K. *Phys. Rev.* **1989**, A40, 1424.
(12) Ohno, K.; Binder, K. *J. Stat. Phys.* **1991**, *64*, 781.
(13) Ohno, K.; Hu, X.; Kawazoe, Y. In *Computer Aided Innovation of New Materials*; Doyama, M., et al., Eds.; Elsevier Scientific Pub.: Amsterdam, 1993; p 143.
(14) Ohno, K. *Macromol. Symp.* **1994**, *81*, 121.
(15) Ohno, K.; Schulz, M.; Binder, K.; Frisch, H. L. *J. Chem. Phys.* **1994**, *101*, 4452.
(16) Lipson, J. E. G.; Whittington, S. G.; Wilkinson, M. K.; Martin, J. L.; Gaunt, D. S. *J. Phys.* **1985**, *A18*, L469.
(17) Wilkinson, M. K.; Gaunt, D. S.; Lipson, J. E. G.; Whittington, S. G. *J. Phys.* **1986**, *A19*, 789.
(18) Batoulis, J.; Kremer, K. *Europhys. Lett.* **1988**, *7*, 683.
(19) Batoulis, J.; Kremer, K. *Macromolecules* **1989**, *22*, 4277.
(20) Ohno, K.; Shida, K.; Kimura, M.; Kawazoe, Y. *Macromolecules* **1996**, *29*, 2269.
(21) Rubio, A. M.; Freire, J. J.; *Macromolecules* **1996**, *29*, 6948.
(22) For example: de Gennes, P. G.; Daoud, M.; Cotton, J. P.; Farnoux, B.; Jannink, G.; Sarma, G.; Benoit, H. *Macromolecules* **1975**, *8*, 804.
(23) Witten, T. A.; Pincus, P. A. *Macromolecules* **1986**, *19*, 2509.
(24) Halperin, A.; Alexander, S. *Macromolecules* **1989**, *22*, 2403.
(25) Merkle, G.; Burchard, W.; Lutz, P.; Freed, K. F.; Gao, J. *Macromolecules* **1993**, *26*, 2736.
(26) Daoud, M.; Cotton, J. P. *J. Phys.* **1982**, *43*, 531.
(27) Fujita, H. *Polymer Solutions*; Elsevier Scientific Pub.: Amsterdam, 1990.
(28) Nakamura, Y.; Norisuye, T.; Teramoto, A. *J. Polym. Sci.: Polym. Phys. Ed.* **1991**, *29*, 153.
(29) Watts, M. G. *J. Phys.* **1975**, *A8*, 61.
(30) Ohno, K. *Phys. Rev. A* **1989**, *40*, 1524.
(31) Okumoto, M.; Terao, K.; Nakamura, Y.; Norisuye, T.; Teramoto, A. *Macromolecules* **1997**, *24*, 77493.
(32) Douglas, J. F.; Roovers, J.; Freed K. F. *Macromolecules* **1990**, *23*, 4168.
(33) Roovers, J.; Hadjichristidis, N.; Fetters, L. *Macromolecules* **1983**, *16*, 214.
(34) Huber, K.; Burchard, W.; Fetters, L. J. *Macromolecules* **1984**, *17*, 541.
(35) Toporowski, P. M.; Roovers, J. *J. Polym. Sci., Polym. Chem. Ed.* **1986**, *24*, 3009.
(36) Raphaël, E.; Pincus, P.; Fredrickson, H. *Macromolecules* **1993**, *26*, 1996.
(37) Croxton, C. A. *Macromolecules* **1993**, *26*, 3572.
(38) Roovers, J. *Macromolecules* **1994**, *27*, 5359.
(39) Shida, K.; Ohno, K.; Kawazoe, Y. *Comput. Theor. Polym. Sci.* **2000**, *10*, 281.

MA990746L